PHILOSOPHICAL TRANSACTIONS OF THE ROYAL SOCIETY A MATHEMATICAL, PHYSICAL & ENGINEERING SCIENCES

Deposition of Diamond-Like Carbon

J. Robertson

Phil. Trans. R. Soc. Lond. A 1993 **342**, 277-286
doi: 10.1098/rsta.1993.0021

Deposition of diamond-like carbon

By J. Robertson

National Power Labs, Leatherhead, Surrey KT22 7SE, U.K.

Diamond-like carbon refers to forms of amorphous carbon and hydrogenated amorphous carbon containing a sizeable fraction of sp^3 bonding, which makes them mechanically hard, infrared transparent and chemically inert. This paper discusses the various thin film deposition processes used to form diamond-like carbon and the deposition mechanisms responsible for promoting the metastable sp^3 bonding.

1. Introduction

Crystalline carbon forms a number of allotropes because the C atom is able to exert both sp^3 and sp^2 hybridization. Graphite, the stable allotrope, is a layered, sp^2-bonded metal. Diamond, only 0.02 eV less stable at 0 K, is a sp^3 bonded, wide band-gap semiconductor with the highest bulk modulus, hardness and atom number density of any solid.

There are also many non-crystalline forms of carbon. The familiar non-crystalline carbons such as soot, evaporated amorphous carbon, or glassy carbon are sp^2 bonded. There is presently great interest in those types of amorphous carbon (a-C) and hydrogenated amorphous carbon (a-C:H) containing significant sp^3 bonding (Angus & Hayman 1988; Robertson 1986, 1991*a*, *b*, 1992*a*). Their sp^3 bonding confer on this 'diamond-like carbon' (DLC) many of the valuable properties of diamond itself, such as high mechanical hardness, low friction, transparency and chemical inertness. In general, DLCs contain a mixture of both sp^3 and sp^2 sites and hydrogen (table 1). They can therefore be considered to be intermediate between diamond, graphite and a polymeric hydrocarbon. This mixed bonding means that their properties are generally poorer than those of diamond. Nevertheless, their low cost, smoothness, low deposition temperature and ability to be deposited on ferrous substrates makes DLC a competitive coating material which is available now. The drawbacks of DLC coatings are their poor thermal stability and high internal stress.

2. Electronic structure

The electronic structure of a-C and a-C:H was reviewed by Robertson (1986, 1991*a*, *b*). Amorphous carbons contain both sp^3 and sp^2 sites. The sp^3 sites form σ bonds while the sp^2 sites form both σ and π bonds. The strong σ bonds form the skeleton of the covalent network. The π bonds favour the segregation of sp^2 sites into graphitic clusters, embedded in a sp^3 bonded matrix. The π states lie closest to the Fermi Level, so they control the electronic properties like the band gap (figure 1). The band gap varies with cluster size as

$$E_g = 6/M^{\frac{1}{2}}\,\mathrm{eV}, \tag{1}$$

where M is the number of six-fold rings in the cluster (Robertson & O'Reilly 1987).

Phil. Trans. R. Soc. Lond. A (1993) **342**, 277–286
Printed in Great Britain

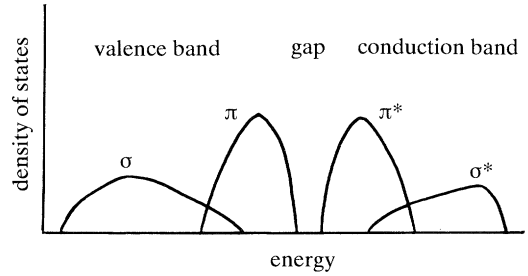

Figure 1. Schematic electronic density of states of amorphous carbons.

Table 1. *Properties of various forms of carbon*

	density	hardness/GPa	sp^3 (%)	H (at. %)	band gap/eV
diamond	3.515	100	100	0	5.5
graphite	2.267	—	0	0	−0.04
glassy C	1.3–1.55	2–3	0	—	0.01
evap a-C	1.8–2.0	2–5	< 5	—	0.4–0.7
MSIB a-C	2.5–3.0	100	90 ± 5	*ca.* 9	1.5–2.5
sput a-C	2.0–2.4	10–14	*ca.* 95	—	*ca.* 0.5
laser nc-C	—	40	—	—	—
hard a-C:H	1.6–2.2	10–40	30–60	20–40	0.8–1.5
soft a-C:H	0.9–1.6	< 5	50–80	40–65	1.5–4
polythene	0.92	0.01	100	67	6

This suggests a two-phase model of amorphous carbons. This model works best for a-C:H, where the sp^3-bonded phase can be a highly cross-linked network as a 'hard' a-C:H, or an open polymeric network as in 'soft' a-C:H. The relatively small band gap, the Raman spectra and the luminescence of a-C:H all support this model (Robertson 1992*b*). The electronic spectra have been studied experimentally by photoemission (Oelhafen *et al.* 1991) and electron energy loss (Fink *et al.* 1983).

3. Mechanical properties

The high hardness, wear resistance and low friction are the most useful valuable properties of DLC. Robertson (1991*b*, 1992*c*, *d*) showed how each of these properties are fundamentally related to the Youngs modulus E, and how E depends on the underlying bonding. The high modulus of diamond results from its strong, directional bonds. The moduli of DLCs are lower because of their finite sp^2 and H content. E is found to vary with mean C–C coordination of the a-C(:H) network, r, as

$$E = E_0\, c_{sp^3}\{(r-2.4)/(r_0-2.4)\}, \tag{2}$$

where E_0 is the modulus of diamond at $r_0 = 4$, and c_{sp^3} is the fraction of sp^3 bonding. The sp^2 fraction of the network tends to contribute no modulus because of its locally layered bonding. Thus, in the two phase model, the Youngs modulus depends only on the sp^3 phase, its concentration and its mean C–C coordination. This model has been found to describe well the modulus of a-C:H, as seen in figure 2. It is less successful for sputtered a-C, whose sizeable modulus of 11–14 GPa (Cho *et al.* 1990) but small sp^3 fraction (*ca.* 5%) implies that there is considerable sp^2-type interlayer cross-linking. The linking may somewhat resemble that in the recently proposed C sponge structures (O'Keeffe *et al.* 1992).

PHILOSOPHICAL TRANSACTIONS OF THE ROYAL SOCIETY A MATHEMATICAL, PHYSICAL & ENGINEERING SCIENCES

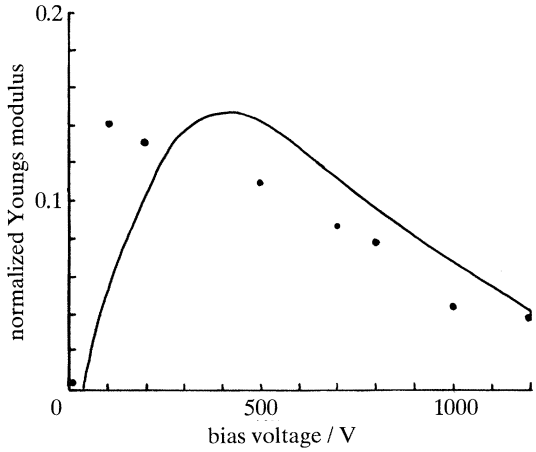

Figure 2. Comparison of experimental (Jiang 1989) and calculated Young's modulus of plasma-deposited a-C:H as a function of bias voltage.

4. Deposition methods

Diamond-like carbon can be prepared by a wide variety of deposition methods, such as ion beam deposition, mass-selected ion beam deposition, ion beam sputtering, magnetron sputtering, plasma deposition and laser plasma deposition. A common feature of each method is the exposure of the growing film to bombardment by ions of medium energy, 20–500 V, which appears necessary to promote sp^3 bonding.

In ion beam deposition, carbon ions are generated by sputtering carbon electrodes by an Ar plasma and then accelerated towards the substrate by a bias electrode. Higher growth rates are possible by generating ions from a hydrocarbon source gas. A solid carbon source gives ions of the form C_m^+, while a hydrocarbon source gives $C_mH_n^+$ ions. In both cases the substrate also receives a large flux of neutral species such as unionized Ar or source gas.

Deposition of a single ion species is possible if the ion beam is passed through a magnetic mass analyser for e/m selection. The analyser filters neutrals, cluster species, graphitic fragments and impurities from the beam and allows only a pure beam of C^+ (or C^-) ions to reach the substrate. This mass-selected ion beam (MSIB) method was first used by Aksenov *et al.* (1970). Structural studies indicate a form of a-C with the highest fraction of sp^3 bonding of those from any present deposition process. The deposition rate for this method can be maximized by using a carbon arc as an ion source. The arc is confined magnetically for stability. The main practical problem with this method is the high compressive stress in the films, which limits adhesion for films over 500 Å† thick (McKenzie *et al.* 1991*a*).

Various sputtering methods can be used. In ion beam sputtering, a beam of typically 1 kV Ar ions is directed at a graphite target. An angle of incidence of 30–45° is used to maximize the yield. A second Ar ion beam can be directed at the substrate to provide bombardment of the growing film. Higher deposition rates can be achieved by magnetron sputtering (Savvides 1990). Here an Ar plasma is used to both sputter from the target and bombard the growing film. Deposition rates are typically 3 Å s^{-1} and increase linearly with RF power. Ion energies are of order 20 eV

† 1 Å = 10^{-10} m = 10^{-1} nm.

and decline slowly with increasing power or gas pressure. The ion/neutral flux ratio falls with increasing sputtering power and gas pressure. The advantage of sputtering is good process control and ease of scale-up to larger apparatus.

One of the most popular methods is RF plasma-deposition (PD) from a hydrocarbon source gas (Koidl *et al.* 1990). RF power is capacitively coupled to the substrate electrode and the counter electrode is either a second electrode or just the grounded walls of the deposition chamber. If the RF frequency is greater than the ion plasma frequency, *ca.* 2–5 MHz, the electrons can follow the RF voltage but the ions cannot. The powered electrode acquires a negative self-bias because of the large difference in electrode size and also in the electron and ion mobilities. The DC bias is largely dropped across an ion sheath in front of the cathode, and it accelerates the ions towards the cathode. The bias voltage V_b varies with RF power W and operating pressure P as $V_b = k(W/P)^{\frac{1}{2}}$. The ion energy E_i depends on V_b and the ion mean free path in the sheath. At low pressures in the absence of collisions $E_i \approx V_b$, while at higher pressures there is a spectrum of ion energies with a mean value of $E_i \approx k' V_b P^{-\frac{1}{2}}$, or $E_b \approx 0.6\ V_b$ for typical pressures of 3 Pa (Koidl *et al.* 1990). The deposition rate for a given source gas tends to vary linearly with bias voltage and gas pressure (Koidl *et al.* 1990; Zou *et al.* 1989, 1990). The rate is highest for gases of low ionization potentials and large molecular weights. Films deposited from acetylene appear to have the best properties, having the highest hardness and a reasonable deposition rate.

A carbon ion plasma can also be produced by the laser ablation of a graphite target (Davanloo *et al.* 1992). The plasma somewhat resembles that formed by a cathodic arc. The resulting film is diamond-like if the laser power exceeds a certain threshold. The DLC is found to consist of nano-scale mixture of diamond grains embedded in an a-C matrix. It has the advantage of high hardness yet moderate internal stress.

The preferred deposition method depends on whether the DLC preparation is for practical application or investigative studies. For practical applications, factors such as deposition rate, film properties, film adherence, sample coverage, process control and scale up are of importance, which favour sputtering, plasma-deposition and ion-plating. MSIB and PD methods are important in fundamental studies.

5. Deposition mechanisms

(*a*) MSIB a-C

A variety of structural measurements (electron energy loss, diffraction) show that MSIB a-C has a high degree (up to 95%) of sp^3 bonding and little hydrogen (McKenzie *et al.* 1991*a*, *b*; Gaskell *et al.* 1991). Figure 3 shows the variation of density with C^+ ion energy, after McKenzie *et al.* (1991*a*). Density is expected to vary closely with sp^3 fraction because of the large density difference between graphite and diamond. The sp^3 fraction increases from 20 eV to reach a peak at about 40 eV before gradually declining at higher energies. Koskinen (1898) and Ishikawa *et al.* (1987) found that other properties such as hardness peak at the same ion energy as density (although they found a higher optimum energy).

The mechanism that promotes sp^3 bonding in a-C is still contentious. Spencer *et al.* (1976) suggested a preferential sputtering of sp^2 sites but Lifshitz *et al.* (1990) noted that this was unlikely due to the low sputtering yield of carbon. Lifshitz *et al.* (1990) proposed a 'subplantation' mechanism in which a preferential displacement of sp^2 sites led to an accumulation of sp^3 sites. This idea was based on estimates of

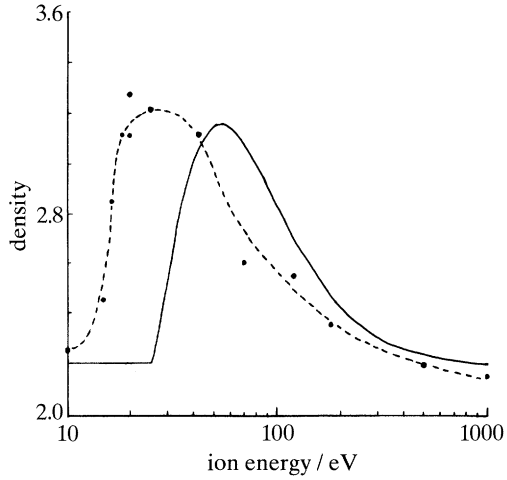

Figure 3. Comparison of experimental (McKenzie *et al.* 1991*b*) and calculated variation of density with ion energy of MSIB a-C. – – –, Experimental; ——, calculated.

the displacement threshold of graphite and diamond as 30 eV and 80 eV respectively. However, recent measurements have found quite similar thresholds for graphite (35 eV, Steffen *et al.* (1992)) and diamond (37–47 eV, Koike *et al.* (1992)), which invalidates this mechanism. McKenzie *et al.* (1991) proposed that the high intrinsic stress moved MSIB a-C into the stability domain of diamond and thereby stabilized sp^3 bonding. Molecular dynamics simulations support a subplantation mechanism (Pailthorpe 1991; Kaukonen & Nieminen 1991).

It is necessary to analyse deposition further in terms of elementary processes to understanding the deposition mechanism. I propose that sp^3 bonding is promoted by the ion flux causing a quenched-in density increase. The bonding hybridization is expected to adjust itself to the local density, becoming more sp^2 at low density and more sp^3 at high density. A high density requires an incident ion to penetrate the first atomic layer of the film and, temporarily, enter an interstitial position. Accumulation of these ions will increase the local density, provided there is little relaxation. The local bonding will reform around the atoms to become bulk bonding of the appropriate hybridization. If the ion energy is too low, the ion fails to penetrate, and it will just stick to the surface and form a sp^2 a-C.

At higher energies, the ion can penetrate further into the solid and increase the density in deeper layers. All penetrating ions will increase the density, in principle. However, the ion must also dissipate its kinetic energy. This energy dissipates quite rapidly in about 10^{-12} s in a 'thermal spike', but it is large and available to activate a relaxation of the excess density. The greater this excess energy, the greater the probability of relaxation. Hence, the optimum ion energy for maximum density is just above the penetration threshold.

Consider a flux F of C ions incident on a growing a-C film (figure 4). Let a fraction f of ions penetrate the surface layer and fraction $(1-f)$ remain on the surface to form sp^2 bonded a-C of density ρ_0. For simplicity, let the ions have a constant range R rather than a distribution. During a time Δt, the film will grow outwards by $\Delta x = F(1-f)\,\Delta t/\rho_0$, while a mass $Ff\Delta t$ of ions is deposited over the same distance Δx, at a depth R below the surface. This increases the local density there by

$$\Delta\rho = \rho_0 f/(1-f). \tag{3}$$

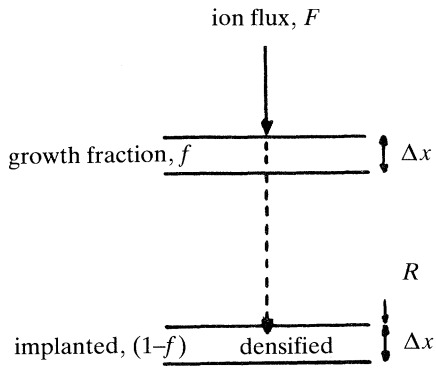

Figure 4. Proposed mechanism for promoting densification and sp^3 bonding by ion beam deposition in a-C.

Now suppose the film density at R can relax during the thermal spikes associated with each ion impact. Let each impact activate n_r atoms for relaxation. The fractional relaxation β is proportional to n_r and β itself, giving $\beta = 1-\beta n_r$ and $\beta = 1/(1+n_r)$. Thus, the density increase including relaxation is

$$\Delta\rho = \rho_0 \beta f/(1-\beta f). \tag{4}$$

This increase sweeps through the film at a depth R below the surface. The same increase occurs if the ion range is a distribution rather than a delta function, the increase is just an integral over the range. An upper layer of depth R remains unconverted with a density ρ_0.

Now consider the ion processes. The ion energies of interest (20–200 eV) are low. At this energy, the ion range is only a few monolayers and energy loss occurs mainly by nuclear stopping. Nuclear stopping consists of elastic collisions between atoms, in which an energy T is transferred to the target atom. The atom is displaced if T exceeds the displacement threshold E_d. E_d is the energy needed to create a permanent Frenkel (vacancy–interstitial) pair by displacement. This exceeds the isothermal Frenkel creation energy by an energy lost in migration and needed to separate the vacancy and interstitial sufficiently to prevent recombination. The Frenkel energies of graphite and diamond are about 15 eV and 21 eV respectively (Thrower & Mayer 1978; Bernholc *et al.* 1988), about half of E_d.

Ion penetration can occur in two ways. First, the ion can pass directly through the surface layer and enter an interstitial site (figure 5*a*). A threshold exists for this process because the collision cross-section increases rapidly at low ion energies. The cross-section diameter exceeds the interatomic separation for ion energies below about 20 eV. The ion range can be calculated by the TRIM code (Biersack & Haggmark 1980). However, this estimate may be questioned as many of the approximations used in TRIM break down at such low energies (Dodson 1990).

Ion penetration can also occur by displacement of an atom in the first layer (figure 5*b*). This requires the ion energy in the solid to exceed E_d. However, the surface is also an attractive potential barrier of height E_B for ions in the solid. E_B the surface binding energy equals the sublimation or cohesive energy, 7.4 eV for C. Thus the net penetration threshold is

$$E_p = E_d - E_B \tag{5}$$

or 28 eV, from $E_d = 35$ eV, $E_B = 7.4$ eV.

PHILOSOPHICAL TRANSACTIONS OF THE ROYAL SOCIETY A MATHEMATICAL, PHYSICAL & ENGINEERING SCIENCES

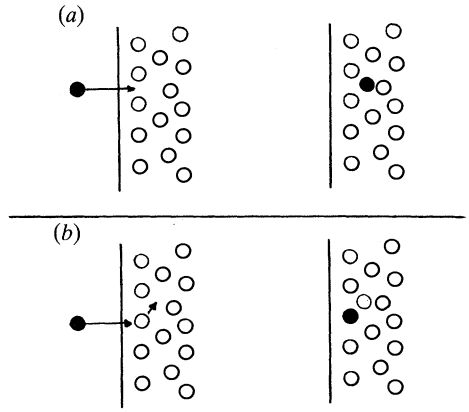

Figure 5. Impact of a low energy ion on a-C, showing (*a*) direct penetration and (*b*) penetration by displacement.

The relaxation of density can be described by the thermal spike model (Seitz & Koehler 1956). Consider a point source of energy Q dissipating by thermal conductivity. The temperature profile is given by

$$T(r,t) = Q/(8\pi^{\frac{3}{2}} c\rho[Dt]^{\frac{3}{2}}) \exp(-r^2/4Dt), \tag{6}$$

where $D = \kappa/c\rho$, ρ is the density, c is the specific heat and κ is the thermal conductivity. Suppose that annealing occurs by a thermal activated process with an attempt frequency

$$v = v_0 \exp(-E'/kT). \tag{7}$$

The total number of jumps within a spike (that is per incident ion) is given by

$$n_r = \int_0^\infty \int_0^\infty v_0 \exp(-E'/kT(r,t)) 4\pi r^2 \,\mathrm{d}r \,\mathrm{d}t. \tag{8}$$

Integration gives $n_r = \{16\Gamma(2/3)/81\pi^{\frac{2}{3}}\} v_0 a^{\frac{2}{3}} (Q/E')$, where $a = (kQ)/(E' c\rho[4\pi D]^{\frac{3}{2}})$, or

$$n_r \approx 0.016(v_0 r_s^2/D)(Q/E')^{\frac{5}{3}}, \tag{9}$$

where $c\rho \approx 3n_0 k$ and $1/n_0 = 4\pi r_s^3$. Most processes occur at early times in the spike when the temperature is very high. Thus, the phonon mean free path is of order of the interatomic spacing r_s, so $D \approx v_0 r_s^2$. This gives

$$n_r \approx 0.016(Q/E')^{\frac{5}{3}}. \tag{10}$$

The ion range at these energies is so low that each ion can be considered to produce a single thermal spike so that $Q \approx E_i$. MSIB *a-C* has a relatively low thermal stability, transforming below $T_t \approx 800C$. This gives $E' = kT_t \ln(v_t) \approx 3.1$ eV, where $v \approx 10^{14}\ \mathrm{s}^{-1}$ and $t \approx 1$ s, the experimental timescale. Note that E' is quite low compared with the C–C bond energy. The density increment can then be calculated using (4) and compared with experiment in figure 3. The agreement is reasonably good, considering the approximations used. The optimum ion energy is found to be $E_i \approx 60$ eV, higher than found by McKenzie *et al.* (1991*a*).

The intrinsic stress of MSIB a-C arises from the high site energy of sp^3 a-C. Kelires (1991) found that the free energy of sp^3 sites in a-C was about 0.3 eV higher

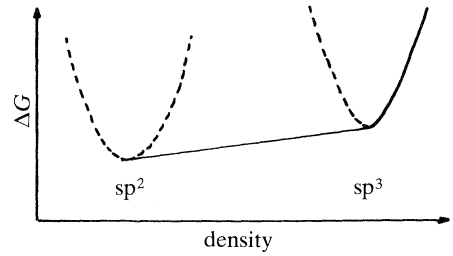

Figure 6. Schematic free energy against density for a-C.

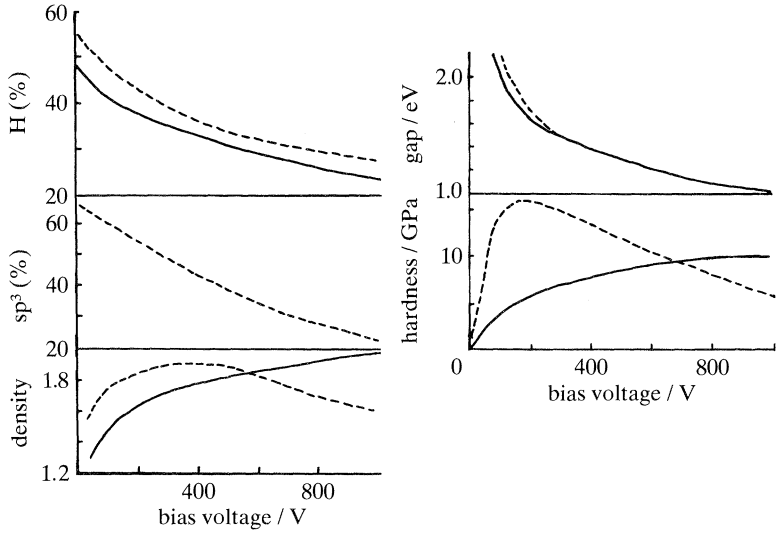

Figure 7. Variation of sp^3 content, H content, density, optical gap and micro-hardness of PD a-C:H deposited from methane (– – –) and benzene (——) (3 Pa pressure); data from Tamor *et al.* (1989, 1991), Koidl *et al.* (1990) and Jiang *et al.* (1989).

than sites in sp^2 a-C network or than diamond and graphite. Figure 6 shows schematically the free energy ΔG of a-C as a function of density. The dashed lines indicate the elastic response of a frozen network, while the full line indicates the ability of a continuously adjustable network to pass from one state to the other. The ion-bombardment model above suggests that the compressive stress P can be viewed as the work done by incident ions in compressing sp^2 sites into sp^3 sites in a disorder network. Thus

$$W = \Delta G = P\,\Delta V. \tag{11}$$

The stress is $P = 15$ GPa for $\Delta G = 0.3$ eV, $\rho_{sp^2} = 2.27$ g cm^{-3}, $\rho_{sp^3} = 3.51$ g cm^{-3}. Smaller density changes give proportionately lower observed stresses.

(*b*) PD a-C:H

The properties of plasma-deposited a-C:H depend primarily on the bias voltage and thus on the mean ion energy E_i. This dependence arises from the variation of the sp^3 and H content with bias (figure 7). The sp^3 and H content both fall with increasing bias (Koidl *et al.* 1990; Tamor *et al.* 1991). This leads to three regimes. At low bias, the high sp^3 and H content produces a polymeric solid, 'soft a-C:H', which is quite soft, light and has a wide band gap. At intermediate bias, the fraction of quaternary carbon (unhydrogenated sp^3 sites) reaches a maximum, giving films of

'hard a-C:H' of the highest density and hardness. At still higher bias, sp^2 bonding becomes dominant which leads to a fall off in density and hardness and a rapid closing of the band gap.

Koidl *et al.* (1990) found that the properties of soft a-C:H depended strongly on source gas, but those of hard a-C:H were not. Koidl attributed this to the complete decomposition of the source gas at high bias, which was incomplete at low bias. This conclusion was partly based on optical emission studies which found a strong signature of the CH radical in both benzene and methane plasmas (Wild & Koild 1987). However, it is now realized that the CH radical is unusually emissive, which can give misleading impressions of plasma dissociation. In fact, Robertson (1991*b*, 1992*a*) found that some properties like density depend strongly on source gas in both soft and hard regimes, while some properties like band gap are almost independent of gas in both regimes, as seen in figure 7.

An alternative model of plasma deposition is now proposed. We first note that while the degree of ionization in the plasma can be high, the degree of decomposition of the source gas is relatively low. Thus, the major ionic species detected by mass spectrometry in ion beams from CH_4, C_2H_4 and C_6H_6 plasmas are CH_3^+, $C_2H_2^+$ and $C_6H_6^+$ ions respectively (Weiler *et al.* 1992; Ehrhardt *et al.* 1992; Schaarschidt *et al.* 1991). Thus, the predominant ion contains the same number of carbon atoms as the source gas molecule. Ions are the major growth species in PD because they have a sticking coefficient of 1. Neutrals do make some contributions to growth, as is clear from comparing growth rates to ion fluxes (see, for example, Locher *et al.* 1991), but we neglect this for the moment. On impact, the molecule ion $C_mH_n^+$ will dissociate into m separate C^+ ions, the energy will be partitioned mainly between the daughter C^+ ions, giving each an energy E_i/m.

Ion bombardment is used to dehydrogenate a-C:H by the preferential sputtering of hydrogen, which is relatively weakly bound. Thus we expected the variation of hydrogen and sp^3 fraction on V_b to scale with source gas as $1/m$. This dependence is indeed found: the maximum density occurs at about $V_b = 300$ eV for a source gas of methane, 500 eV for acetylene and over 1000 eV for benzene (figure 7).

In contrast, the bias dependence of band gap is independent of source gas. In this case the band gap depends on the sp^2 site fraction and their clustering (Robertson & O'Reilly 1987). sp^2 sites are formed mainly by thermally activated elimination

$$=CH—CH= \rightarrow =C=C= + H_2.$$

The sp^2 sites are likely to be formed by this reaction in a thermal spike. Now, although a molecular ion may dissociate on impact, partitioning its energy between m daughter ions, each ion will loose its energy within the same small region, within the same thermal spike. Thus, we expect properties depending on the sp^2 sites to be independent of m of the source gas, as is indeed seen in figure 7.

The author is very grateful to Dr A. Fuchs and Professor H. Ehrhardt for discussions and performing TRIM calculations.

References

Angus, J. C. & Hayman, C. C. 1988 *Science, Wash.* **241**, 913.

Aksenov, I. I., Vakula, S. I., Padalka, V. G., Strelnitski, R. E. & Khoroshikh, V. M. 1980 *Soviet Phys. tech. Phys.* **25**, 1164.

Bernholc, J., Antonelli, A., DelSole, T. M., BarYam, Y. & Pantelides, S. T. 1988 *Phys. Rev. Lett.* **61**, 2693.

Biersack, J. P. & Haggmark, L. G. 1980 *Nucl. Instr. Methods* **174**, 257.
Davanloo, F., Lee, T. J., Jander, D. R., Park, H. & Collins, C. B. 1992 *J. appl. Phys.* **71**, 1446.
Dodson, B. W. 1989 *Mater. Res. Soc. Symp. Proc.* **128**, 137.
Ehrhardt, H. *et al.* 1992 *Diamond Related Mater.* **1**, 316.
Fink, J. *et al.* 1983 *Solid State Commun.* **47**, 887.
Gaskell, P. H., Saeed, A., Chieux, P. C. & McKenzie, D. R. 1991 *Phys. Rev. Lett.* **67**, 1286.
He, H. & Thorpe, M. F. 1985 *Phys. Rev. Lett.* **54**, 2107.
Ishikawa, J., Takeiri, Y., Ogawa, K. & Takagi, T. 1987 *J. appl. Phys.* **61**, 2509.
Jiang, X., Reichelt, K. & Stritzker, B. 1989 *J. appl. Phys.* **66**, 5805.
Kaukonen, H. P. & Nieminen, R. M. 1992 *Phys. Rev. Lett.* **68**, 620.
Kelires, P. C. 1992 *Phys. Rev. Lett.* **68**, 1854.
Koidl, P., Wild, C., Dischler, B., Wagner, J. & Ramsteiner, M. 1990 *Mater. Sci. Forum* **52**, 41.
Koike, J., Parkin, D. M. & Mitchell, T. E. 1992 *Appl. Phys. Lett.* **60**, 1450.
Koskinen, J. 1988 *J. appl. Phys.* **63**, 2094.
Lifshitz, Y., Kasi, S. R., Rabalais, J. W. & Eckstein, W. 1990 *Phys. Rev.* B**41**, 10468.
Locher, R., Wild, C. & Koidl, P. 1991 *Surf. Coatings Technol.* **47**, 426.
McKenzie, D. R. *et al.* 1991*a* *Diamond Related mater.* **1**, 51.
McKenzie, D. R., Muller, D. & Pailthorpe, B. A. 1991*b* *Phys. Rev. Lett.* **67**, 773.
O'Keeffe, M., Adams, G. B. & Sankey, O. F. 1992 *Phys. Rev. Lett.* **68**, 2325.
Oelhafen, P., Ugolini, D., Schelz, S. & Eitle, J. 1991 In *Diamond and diamond-like carbon films* (ed. R. E. Clausing *et al.*), p. 377. Plenum.
Pan, H., Pruski, M., Gerstein, B. C., Li, F. & Lannin, J. S. 1991 *Phys. Rev.* B**44**, 6741.
Pailthorpe, B. A. 1991 *J. appl. Phys.* **70**, 543.
Robertson, J. 1986 *Adv. Phys.* **35**, 317.
Robertson, J. 1991*a* In *Diamond and diamond-like carbon films* (ed. R. E. Clausing *et al.*), p. 331. Plenum.
Robertson, J. 1991*b* *Prog. Solid State Chem.* **21**, 199.
Robertson, J. 1992*a* *Surf. Coatings Technol.* **50**, 185.
Robertson, J. 1992*b* *Phil. Mag.* B**66**, 199.
Robertson, J. 1992*c* *Phys. Rev. Lett.* **68**, 220.
Robertson, J. 1992*d* *Diamond Related Mater.* **1**, 397.
Robertson , J. & O'Reilly, E. P. 1987 *Phys. Rev.* B**35**, 2946.
Savvides, N. 1990 *Mater. Res. Forum* **52**, 407.
Schaarschidt, G. *et al.* 1991 *Mater. Sci. Engng* A**140**, 788.
Seitz, F. & Koehler, J. S. 1956 In *Solid state physics* (ed. F. Seitz & D. Turnbull), vol. 2, p. 305.
Spencer, E. G., Schidt, P. H., Joy, D. C. & Salasone, F. J. 1976 *Appl. Phys. Lett.* **29**, 118.
Steffen, H. J., Marton, D. & Rabalais, J. E. 1992 *Phys. Rev. Lett.* **68**, 1726.
Tamor, M. A., Haire, J. A., Wu, C. H. & Hass, K. C. 1989 *Appl. Phys. Lett.* **54**, 123.
Tamor, M. A., Vassell, W. C. & Carduner, K. R. 1991 *Appl. Phys. Lett.* **58**, 592.
Thrower, P. A. & Mayer, R. M. 1978 *Phys. Status Solidi* A**47**, 11.
Weiler, M., Kleber, R., Jung, K. & Ehrhardt, H. 1992 *Diamond Related Mater.* **1**, 121.
Wild, C. & Koidl, P. 1987 *Appl. Phys. Lett.* **51**, 1506.
Zou, J. W., Reichelt, K., Schmidt, K. & Dischler, B. 1989 *J. appl. Phys.* **65**, 3914.
Zou, J. W., Schmidt, K., Reichelt, K. & Dischler, B. 1990 *J. appl. Phys.* **67**, 487.

PHILOSOPHICAL TRANSACTIONS OF THE ROYAL SOCIETY A MATHEMATICAL, PHYSICAL & ENGINEERING SCIENCES